Macrocyclic Cu^{II}_2, Cu^{II}_4, Ni^{II}_3, and Ni^{II}_4 Complexes: Magnetic Properties of Tetranuclear Systems

Sasankasekhar Mohanta,[†] Kausik K. Nanda,[†] Rüdiger Werner,[‡] Wolfgang Haase,[‡] Alok K. Mukherjee,[§] Sujit K. Dutta,[†] and Kamalaksha Nag*,[†]

Department of Inorganic Chemistry, Indian Association for the Cultivation of Science, Calcutta 700 032, India, Institut für Physikalische Chemie der Technischen Hochschule Darmstadt, D-64287 Darmstadt, Germany, and Department of Physics, Jadavpur University, Calcutta 700 032, India

Received September 11, 1996[⊗]

A binuclear tetraprotonated macrocyclic complex $[Mg_2(L^2\text{-}H_4)(NO_3)_2](NO_3)_2\cdot 6H_2O$ (**1**) has been obtained by template condensation of 4-methyl-2,6-diformylphenol and 1,2-diaminoethane in the presence of magnesium acetate and nitrate. Complex **1** on reduction with $NaBH_4$, followed by the removal of magnesium, yields the 36-membered octaaminotetraphenol macrocyclic ligand H_4L^1. The replacement of magnesium in **1** with copper(II) leads to the formation of the binuclear complex $[Cu_2L^3(ClO_4)_2]$ (**2**) derived from the [2+2] cyclization product of 4-methyl-2,6-diformylphenol and 1,2-diaminoethane. From H_4L^1 a series of tetranuclear nickel(II) complexes **5**−**8** with the core cation $[Ni_4L^1(\mu_2\text{-}X)_2(\mu_2\text{-}H_2O)_2]^{2+}$ (X = NCS, N_3, OAc, or Cl) have been synthesized and characterized. The trinuclear complex $[Ni_3L^1(acac)_2(H_2O)_2\cdot 2H_2O$ (**9**), obtained by reacting nickel(II) acetylacetonate with H_4L^1, on treatment with nickel(II) perchlorate produces the tetranuclear compound $[Ni_4L^1(acac)_2(H_2O)_4](ClO_4)_2$ (**10**). Variable-temperature (4−300 K) magnetic susceptibility measurements have been carried out for the tetracopper(II) complex $[Cu_4L^1(H_2O)_4](ClO_4)_4$ (**3**) and the tetranickel(II) complexes $[Ni_4L^1(\mu_3\text{-}OH)(\mu_2\text{-}H_2O)_2(ClO_4)](ClO_4)_2\cdot 2CH_3COCH_3\cdot H_2O$ (**4**), $[Ni_4L^1(\mu_2\text{-}NCS)_2(\mu_2\text{-}H_2O)_2](ClO_4)_2\cdot 2CH_3CN$ (**5**), $[Ni_4L^1(\mu_2\text{-}N_3)_2(\mu_2\text{-}H_2O)_2](ClO_4)_2\cdot 2CH_3OH$ (**6**), $[Ni_4L^1(\mu_2\text{-}OAc)_2(\mu_2\text{-}H_2O)_2](ClO_4)_2\cdot 2H_2O$ (**7**), and $[Ni_4L^1(\mu_2\text{-}Cl)_2(\mu_2\text{-}H_2O)_2]Cl_2\cdot 4H_2O$ (**8**). The X-ray structure of **5** has been determined. The complex ($C_{50}H_{70}N_{12}O_{14}Cl_2S_2Ni_4$) crystallizes in the triclinic space group $P\bar{1}$ with $a = 11.794(6)$ Å, $b = 12.523(4)$ Å, $c = 12.794(5)$ Å, $\alpha = 117.28(5)°$, $\beta = 96.38(4)°$, $\gamma = 109.65(3)°$, and $Z = 1$. In the asymmetric unit each of the nickel(II) centers with distorted octahedral geometry is triply-bridged by a phenoxide group, a water molecule, and a N-bonded thiocyanate and these metal centers are further bridged to their symmetry-related counterparts by another phenoxide group. The experimental susceptibility data have been analyzed using appropriate Heisenberg spin coupling models ($H = -2\sum_{j>i=1}^{4} J_{ij}S_i\cdot S_j$) and the best-fit spin exchange parameters obtained are as follows: $J = -288(3)$ cm^{-1} (**3**); $J_1 = -8.1(2)$ cm^{-1}, $J_2 = -10.2(2)$ cm^{-1} (**4**); $J_1 = -34.5(1.0)$ cm^{-1}, $J_2 = -9.5(2.0)$ cm^{-1} (**5**); $J_1 = -34(1)$ cm^{-1}, $J_2 = 11(2)$ cm^{-1} (**6**); $J_1 = -30(1)$ cm^{-1}, $J_2 = -7.0(1.5)$ cm^{-1} (**7**); $J_1 = -32(1)$ cm^{-1}, $J_2 = -4(1)$ cm^{-1} (**8**).

Introduction

Magnetic exchange interactions in bimetallic complexes have elicited interest of chemists for a long time. The sign and magnitude of exchange coupling constant (J) can be qualitatively predicted in terms of energetics and overlap of magnetic orbitals.[1−3] A few quantitative magneto-structural correlations have emerged for certain types of binuclear complexes of copper(II),[4,5a,6] nickel(II),[7−9] chromium(III),[10−12] and iron(III).[13] The focus of attention has now shifted to understand magnetic properties of high-nuclearity metal complexes[14−16] as they hold promise for molecular magnetic materials.

A major problem to deal with polymetallic compounds is computation of energies of large number of eigenstates of spin Hamiltonian that are required for evaluation of exchange coupling constants. Often J values of tri- and tetranuclear systems are calculated by generalized vector coupling method[17] proposed by Kambe.[18] However, applicability of this method is restricted to systems where the paramagnetic centers are arranged in certain symmetric ways. A more rigorous treatment demands exact diagonalization of the effective spin Hamiltonian, which becomes nontrivial as the dimension of the matrix

[†] Indian Association for the Cultivation of Science.
[‡] Technische Hochschule Darmstadt.
[§] Jadavpur University.
[⊗] Abstract published in *Advance ACS Abstracts,* August 15, 1997.

(1) Kahn, O. *Molecular Magnetism*; VCH Publications: New York, 1993.
(2) Willet, R. D., Gatteschi, D., Kahn, O., Eds. *Magneto-Structural Correlation in Exchange Coupled Systems*; D. Reidel: Dordrecht, The Netherlands, 1985.
(3) Ginsberg, A. P. *Inorg. Chim. Acta Rev.* **1971**, *5*, 45.
(4) Crawford, V. M.; Richardson, M. W.; Wasson, J. R.; Hodgson, D. J.; Hatfield, W. E. *Inorg. Chem.* **1976**, *19*, 173.
(5) (a) Merz, L.; Haase, W. *J. Chem. Soc., Dalton Trans.* **1980**, 875. (b) Gehring, S.; Fleischhauer, P.; Paulus, H.; Haase, W. *Inorg. Chem.* **1993**, *32*, 54.
(6) Livermore, J. C.; Willet, R. D.; Gaura, R. M.; Landee, C. P. *Inorg. Chem.* **1982**, *21*, 1403.
(7) Nanda, K. K.; Thompson, L. K.; Bridson, J. N.; Nag, K. *J. Chem. Soc., Chem. Commun.* **1994**, 1337.
(8) Wang, C.; Fink, K.; Staemmler, V. *Chem. Phys.* **1995**, *192*, 25.
(9) (a) Ribas, J.; Monfort, M.; Diaz C.; Bastos, C.; Solans, X. *Inorg. Chem.* **1993**, *32*, 3557. (b) Escuer, A.; Vicente, R.; Ribas, J.; El Fallah, M. S.; Solans, X.; Font-Bardia, M. *Inorg. Chem.* **1993**, *32*, 3727.
(10) Glerup, J.; Hodgson, D. J.; Pederson, E. *Acta Chem. Scand.* **1983**, *A37*, 161.
(11) Niemann, A.; Bossek, U.; Wieghardt, K.; Butzliaff, C.; Trautwein, A. X.; Nuber, B. *Angew. Chem., Int. Ed. Engl.* **1992**, *31*, 311.
(12) Spiccia, L.; Fallon, G. D.; Markiewicz, A.; Murray, K. S.; Reisen, H. *Inorg. Chem.* **1992**, *31*, 1066.
(13) Gorun, S. M.; Lippard, S. J. *Inorg. Chem.* **1991**, *30*, 1625.
(14) Gatteschi, D., Kahn, O., Miller, J. S., Palacio, F., Eds. *Magnetic Molecular Materials*; Kluwer Academic Publishers: Dordecht, The Netherlands, 1991.
(15) O'Connor, C. J., Ed. *Research Frontiers in Magnetochemistry*; World Scientific: Singapore, 1993.
(16) Gatteschi, D.; Caneschi, A.; Pardi, L.; Sessoli, R. *Science* **1994**, *265*, 1054.
(17) Sinn, E. *Coord. Chem. Rev.* **1970**, *5*, 313.
(18) Kambe, K. *J. Phys. Soc. Jpn.* **1950**, *5*, 48.

S0020-1669(96)01110-X CCC: $14.00

$\prod_{i=1}^{n}(2S_i + 1)$ gets very large with the increase of the number of nuclei (n) and there spin values (S_i). Nevertheless, over the past few years considerable insight has been obtained on the magnetic properties of several high-nuclearity metal complexes.[14−16,19−30]

Among various bridged complexes, superexchange mediated through phenoxide bridges have been extensively studied.[31] A number of phenoxo-bridged polymetallic complexes obtained by template condensation reactions involving 4-methyl-2,6-diformylphenol and diamines or diamino alcohols or diaminophenols have been reported.[30,32−36] In a preliminary communication we have reported[37] the synthesis of the 36-membered octaaminotetraphenol macrocyclic ligand H_4L^1 (Chart 1) and the structure of the tetranuclear nickel(II) complex $[Ni_4L^1(\mu_3\text{-}OH)(\mu_2\text{-}H_2O)_2(ClO_4)](ClO_4)_2\cdot 2CH_3COCH_3\cdot H_2O$. We now report further developments of the nickel(II) chemistry and the variable-temperature magnetic properties of the series $[Ni_4L^1(\mu_2\text{-}X)_2(\mu_2\text{-}H_2O)_2](ClO_4)_2\cdot$solvent (where X = NCS, N_3, or OAc), $[Ni_4L^1(\mu_2\text{-}Cl)_2(\mu_2\text{-}H_2O)_2]Cl_2\cdot 4H_2O$, $[Ni_4L^1(\mu_3\text{-}OH)(\mu_2\text{-}H_2O)_2ClO_4)](ClO_4)_2\cdot$solvent, and the tetracopper(II) complex $[Cu_4L^1(H_2O)_4](ClO_4)_4$. We also report that the magnesium(II) complex complex $[Mg_2(L^2\text{-}H_4)(NO_3)_2](NO_3)_2\cdot 6H_2O$, obtained by [4+4] condensation reaction between 4-methyl-2,6-diformylphenol and 1,2-diaminoethane, on transmetalation with copper(II) perchlorate produces the binuclear complex $[Cu_2L^3(ClO_4)_2]$.

Chart 1

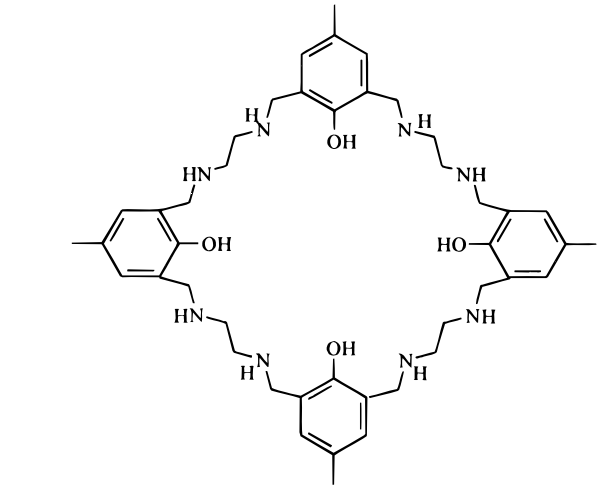

H_4L^1

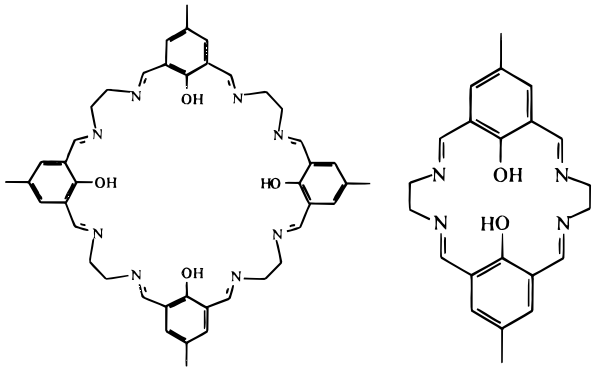

H_4L^2 H_2L^3

Experimental Section

All reagents and solvents were purchased from commercial sources and used as received. 4-Methyl-2,6-diformylphenol was prepared by a reported method.[38] Elemental (C, H, and N) analyses were performed on a Perkin-Elmer 2400II analyzer, while nickel was analyzed gravimetrically as the dimethylglyoximate.

Synthesis. $[Mg_2(L^2\text{-}H_4)(NO_3)_2](NO_3)_2\cdot 6H_2O$ (1). A methanol solution (300 mL) of 4-methyl-2,6-diformylphenol (4.92 g, 30 mmol), $Mg(OAc)_2\cdot 4H_2O$ (3.21 g, 15 mmol), and $Mg(NO_3)_2\cdot 6H_2O$ (3.84 g, 15 mmol) was first heated under reflux for 15 min, to which was slowly added a methanol solution (120 mL) of 1,2-diaminoethane (1.80 g, 30 mmol) over a period of 4 h. After refluxing for another 4 h, the orange yellow magnesium(II) complex that deposited was filtered off, washed with methanol and chloroform, and dried in air; yield 6.5 g (75%). Anal. Calcd for $C_{44}H_{60}N_{12}O_{22}Mg_2$: C, 45.67; H, 5.19; N, 14.53. Found: C, 46.07; H, 4.97; N, 14.29. ^{1}H NMR (DMSO-d_6): 2.18 (s, 12H, CH_3), 3.96 (s, 16H, CH_2CH_2), 7.44 (s, 8H, C_6H_2), 8.50 (s, 8H, CH═N).

H_4L^1. The method of preparation reported earlier[37] has been modified to obtain improved yield. To a suspension of **1** (4.65 g, 4 mmol) in methanol (150 mL), cooled to about 15 °C, was added solid $NaBH_4$ (4.0 g) in small portions over a period of 1 h. Stirring was continued for 1 h more, and the colorless solution that resulted was filtered to remove any suspended material. The filtrate was diluted with water (500 mL), acidified (pH ≈ 2) with HCl (4 M), and mixed with an aqueous solution (200 mL) of the disodium salt of ethylenediaminetetraacetic acid (Na_2H_2EDTA, 10 g) and aqueous ammonia (50 mL). The solution was then extracted with chloroform (3 × 200 mL). The combined organic layer, after washing with water and drying (Na_2SO_4), was rotary evaporated nearly to dryness. The product was

(19) Caneschi, A.; Gatteschi, D.; Laugier, J.; Rey, P.; Sessoli, R.; Zanchi, C. *J. Am. Chem. Soc.* **1988**, *110*, 2795.
(20) Aussoleil, J.; Cassoux, P.; Loth, P.; Tuchagues, J.-P. *Inorg. Chem.* **1989**, *28*, 3051.
(21) Barra, A. L.; Gatteschi, D.; Müller, A.; Doring, J. *J. Am. Chem. Soc.* **1992**, *114*, 8509.
(22) Sessoli, R.; Tsai, H.-L.; Shake, A. R.; Wang, S.; Vincent, J. B.; Folting, K.; Gatteschi, D.; Christou, G.; Hendrickson, D. N. *J. Am. Chem. Soc.* **1993**, *115*, 1804.
(23) Delfs, C.; Gatteschi, D.; Pardi, L.; Sessoli, R.; Wieghardt, K.; Hanh, D. *Inorg. Chem.* **1993**, *32*, 3099.
(24) Taft, K. L.; Delfs, C.; Papaefthymiou, G. C.; Foner, S.; Gatteschi, D.; Lippard, S. J. *J. Am. Chem. Soc.* **1994**, *116*, 823.
(25) Real, J. A.; Munno,G. D.; Chiapetta, R.; Julve, M.; Lloret, F.; Journeaux, Y.; Colin, J. C.; Blondin, G. *Angew. Chem., Int. Ed. Engl.* **1994**, *33*, 1184.
(26) Blake, A. J.; Grant, C. M.; Parsons, S.; Rawson, J. M.; Winpenny, R. E. P. *J. Chem. Soc., Chem. Commun.* **1994**, 2363.
(27) Krebs, C.; Winter, M.; Weyhermüller, I.; Bill, E.; Wieghardt, K.; Chaudhuri, P. *J. Chem. Soc., Chem. Commun.* **1995**, 1913.
(28) Halcrow, M. A.; Sun, J.-S.; Huffman, J. C.; Christou, G. *Inorg. Chem.* **1995**, *34*, 4167.
(29) Kruger, P. E.; Fallon, G. D.; Moubarakai, B.; Berry, K. J.; Murray, K. S. *Inorg. Chem.* **1995**, *34*, 4808.
(30) Tandon, S. S.; Thompson, L. K.; Bridson, J. N.; Benelli, C. *Inorg. Chem.* **1995**, *34*, 5507.
(31) For references, see: Nanda, K. K.; Dutta, S. K.; Baitalik, S.; Venkatsubramanian, K.; Nag, K. *J. Chem. Soc., Dalton Trans.* **1995**, 1239.
(32) (a) Mckee, V.; Tandon, S. S. *J. Chem. Soc., Chem. Commun.* **1988**, 385; **1988**, 1334. (b) Mckee, V.; Tandon, S. S. *Inorg. Chem.* **1989**, *28*, 2901. (c) Tandon, S. S.; Mckee, V. *J. Chem Soc., Dalton Trans.* **1989**, 19; **1991**, 2901.
(33) (a) Bell, M.; Edwards, A. J.; Hoskins, B. F.; Kachab, E. H.; Robson, R. *J. Am. Chem. Soc.* **1989**, *111*, 3603. (b) Hoskins, B. F.; Robson, R.; Smith, P. *J. Chem. Soc., Chem. Commun.* **1990**, 488. (c) Grannas, M. J.; Hoskins, B. F.; Robson, R. *J. Chem. Soc., Chem. Commun.* **1990**, 1644. (d) Edwards, A. J.; Hoskins, B. F.; Kachab, E. H.; Markiewicz, A.; Murray, K. S.; Robson, R. *Inorg. Chem.* **1992**, *31*, 3585.
(34) (a) Tandon, S. S.; Thompson, L. K.; Bridson, J. N. *J. Chem. Soc., Chem. Commun.* **1992**, 911. (b) Tandon, S. S.; Thompson, L. K.; Bridson, J. N.; Mckee, V.; Downard, A. J. *Inorg. Chem.* **1992**, *31*, 4635.
(35) Sakiyama, H.; Motoda, K.-I.; Okawa, H.; Kida, S. *Chem. Lett.* **1991**, 1133.
(36) Nanda, K. K.; Dutta, S. K.; Adhikary, B. *Indian J. Chem.* **1995**, *34A*, 64.
(37) Nanda, K. K.; Venkatsubramanian, K.; Majumdar, D.; Nag, K. *Inorg. Chem.* **1994**, *33*, 1581.
(38) Ullman, F.; Brittner, K. *Chem. Ber.* **1909**, *42*, 2539.

recrystallized from chloroform−methanol (1:1) mixture; yield 2.75 g (90%); Mp 158 °C; ^{1}H NMR ($CDCl_3$) 2.20 (s, 12H, CH_3), 2.74 (s, 16H, CH_2CH_2), 3.80 (s, 24H, $ArCH_2NH$), 6.80 (s, 8H, C_6H_2); ^{13}C NMR ($CDCl_3$) 20.44 (CH_3), 47.90 (CH_2), 50.84 (CH_2), 124.28 (4-C_6H_2), 127.48 (2,6-CH_2), 128.80 (3,5-C_6H_2), 151.16 (1-C_6H_2).

$[Cu_2L^3(ClO_4)_2]$ (2). A mixture of **1** (0.58 g, 0.5 mmol), $Cu(ClO_4)_2\cdot 6H_2O$ (0.74 g, 2 mmol), and triethylamine (0.2 g, 2 mmol) in methanol (50 mL) was refluxed for 1 h. During this period a chocolate brown product (**2**) deposited, which was collected by filtration. The compound was recrystallized from a DMF−MeOH mixture; yield 0.53 g (75%). Anal. Calcd for $C_{22}H_{22}N_4O_{10}Cl_2Cu_2$: C, 37.70; H, 3.14; N, 8.00. Found: C, 38.02; H, 3.21; N, 8.12.

$[Cu_4L^1(H_2O)_4](ClO_4)_4$ (3). The preparation of this compound has been reported elsewhere.[39]

$[Ni_4L^1(\mu_3\text{-}OH)(\mu_2\text{-}H_2O)_2(ClO_4)](ClO_4)_2\cdot 2CH_3COCH_3\cdot H_2O$ (4). The method of prepartion has been already reported.[37]

$[Ni_4L^1(\mu_2\text{-}NCS)_2(\mu_2\text{-}H_2O)_2](ClO_4)_2\cdot 2CH_3CN$ (5), $[Ni_4L^1(\mu_2\text{-}N_3)_2(\mu_2\text{-}H_2O)_2](ClO_4)_2\cdot 2CH_3OH$ (6), and $[Ni_4L^1(\mu_2\text{-}OAc)_2(\mu_2\text{-}H_2O)_2](ClO_4)_2\cdot 2H_2O$ (7). All these compounds were prepared in the same way as illustrated below for **6** except that NaN_3 was replaced with equimolar quantities of NaOAc or NaNCS.

Complex **4** (0.74 g, 0.5 mmol) dissolved in a mixture of methanol (30 mL) and acetonitrile (20 mL) was treated with an aqueous solution (5 mL) of NaN_3 (0.26 g, 4 mmol). The solution was refluxed for 0.5 h and reduced in volume to *ca*. 15 mL. On standing, sky blue crystals of **6** deposited, which were collected by filtration and recrystallized from methanol−acetonitrile (1:1) mixture; 0.59 g (85%). Anal. Calcd for $C_{46}H_{72}N_{14}O_{16}Cl_2Ni_4$ (**6**): C, 39.97; H, 5.21; N, 14.19; Ni, 16.99. Found: C, 39.84; H, 5.29; N, 14.03; Ni, 17.10. Calcd for $C_{50}H_{70}N_{12}O_{14}Cl_2S_2Ni_4$ (**5**): C, 41.90; H, 4.88; N, 11.73; Ni, 16.40. Found: C, 41.68; H, 4.96; N, 11.61; Ni, 16.28. Calcd for $C_{48}H_{74}N_8O_{20}Cl_2Ni_4$ (**7**): C, 41.50; H, 5.33; N, 8.07; Ni, 16.90. Found: C, 41.66; H, 5.24; N, 8.15; Ni, 17.01. For complexes **5** and **7** yields were *ca*. 80%.

$[Ni_4L^1(\mu_2\text{-}Cl)_2(\mu_2\text{-}H_2O)_2]Cl_2\cdot 4H_2O$ (8). $NiCl_2\cdot 6H_2O$ (0.95 g, 4 mmol) and H_4L^1 (0.78 g, 1 mmol) were dissolved in methanol (30 mL), and to the solution was added triethylamine (0.404 g, 4 mmol). The solution was refluxed for 15 min, after which it was allowed to evaporate at room temperature. The blue crystalline solid that deposited was filtered off and recrystallized from ethanol; yield 0.94 g (75%). This compound can be prepared alternatively by reacting **4** with LiCl. Anal. Calcd for $C_{44}H_{72}N_8O_{10}Cl_4Ni_4$: C, 42.27; H, 5.76; N, 8.97; Ni, 18.80. Found: C, 42.10; H, 5.66; N, 9.05; Ni, 18.72.

$[Ni_3L^1(acac)_2(H_2O)_2]\cdot 2H_2O$ (9). Nickel(II) acetylacetonate (0.77 g, 3 mmol) and H_4L^1 (0.77 g, 1 mmol) were dissolved in methanol (100 mL), and the solution was refluxed for 1 h. A red solution that formed initially turned green in a few minutes, and eventually green crystals of **9** deposited. The product was filtered off and recrystallized from chloroform−methanol (1:1) mixture; yield 1.1 g (90%). Anal. Calcd for $C_{54}H_{82}N_8O_{12}Ni_3$: C, 53.54; H, 6.77; N, 9.25; Ni, 14.55. Found: C, 53.42; H, 6.63; N, 9.12; Ni, 14.39.

$[Ni_4L^1(acac)_2(H_2O)_4](ClO_4)_2$ (10). To a boiling suspension of **9** (0.60 g, 0.5 mmol) in methanol (50 mL) was added solid $Ni(ClO_4)_2\cdot 6H_2O$ (0.18 g, 0.5 mmol). In a short while a clear green solution was obtained, which on slow evaporation gave emerald crystals. Separation of these crystals from the mother liquor lead to immidiate crumbling into powder; yield 0.62 g (85%). Anal. Calcd for $C_{45}H_{82}N_8O_{20}Cl_2Ni_4$: C, 44.14; H, 5.58; N, 7.63; Ni, 16.0. Found: C, 44.32; H, 5.65; N, 7.52; Ni, 16.15.

Safety Note. *Perchlorate salts are potentially explosive and should be handled in small quantities.* No problems were encountered with the complexes reported in this study.

Physical Methods. IR spectra were recorded on a Perkin-Elmer 783 spectrophotometer using KBr disks. Electronic absorption spectra were obtained with Shimadzu UV 2100 and Hitachi U3400 spectrophotometers over the UV−vis and near-IR regions. NMR spectra were obtained on a Bruker AC 250 spectrometer. The cyclic voltammetric and differential pulse voltammetric measurements were carried out in dimethyl sulfoxide (DMSO) solutions with tetraethylammonium perchlorate (TEAP, 0.1 M) as the supporting electrolyte using a BAS 100B electrochemical analyzer. A three-electrode assembly (BAS) comprising a glassy carbon or platinum disk working electrode, a platinum auxiliary electrode, and a Ag/AgCl reference electrode were used. The reference electrode was seperated from the bulk solution with a salt bridge having a Vycor plug. Under the experimental condition the ferrocene/ferrocenium couple was observed at 0.38 V.

Magnetic susceptibility of powdered samples were recorded on a Faraday-type magnetometer using a Cahn RG electrobalance in the temperature range 4−300 K. The magnetic field applied was ≈1.2 T. Details of the apparatus have been described elsewhere.[5] Experimental susceptibility data were corrected for diamagnetism using Pascal's constants.[40]

Table 1. Crystallographic Data for $[Ni_4L^1(\mu_2\text{-}NCS)_2(\mu_2\text{-}H_2O)_2](ClO_4)_2\cdot 2CH_3CN$ (**5**)

formula	$C_{50}H_{70}N_{12}Cl_2Ni_4O_{14}S_2$	V, Å^3	1500.1(11)
fw	1432.4	Z	1
space group	$P\bar{1}$	λ(Mo Kα)	0.71073
a, Å	11.794(6)	μ, mm^{-1}	1.467
b, Å	12.523(4)	ρ_{calcd}, g cm^{-3}	1.586
c, Å	12.794(5)	T, °C	20
α, deg	117.28(3)	$R1$,[a] $wR2$[b]	0.0832,
β, deg	96.38(4)	($I > 2\sigma(I)$)	0.1966
γ, deg	109.65(3)	$R1$, $wR2$	0.1181,
		(all data)	0.2303

[a] $R1 = [\sum||F_o| - |F_c||/\sum|F_o|]$. [b] $wR2 = [\sum w(F_o^2 - F_c^2)^2/\sum w(F_o^2)^2]^{1/2}$.

Crystal Structure Determination of $[Ni_4L^1(\mu_2\text{-}NCS)_2(\mu_2\text{-}H_2O)_2](ClO_4)_2\cdot 2CH_3CN$ (5). Crystals suitable for structure determination were obtained by diffusing diethyl ether to a solution of **5** in acetonitrile−methanol (1:1) mixture.

Diffraction data were collected on a Siemens R3m/V diffractometer in the $\omega-2\theta$ scan mode using graphite-monochromatized Mo Kα radiation. Pertinent crystallographic data are summarized in Table 1. Three standard reflections were periodically monitored, and no crystal decay was observed. The intensity data were corrected for Lorentz and polarization effects and semiempirical absorption correction was made from ψ-scans. A total of 3546 reflections were collected in the range $2\theta = 4-45°$, with $h = 0$ to 12, $k = -13$ to 12, and $l = -13$ to 13, of which 3314 reflections were considered independent ($R_{int} = 0.0505$) and 3289 data were used for structure determination. Due to rather irregular shape of the crystal, search routine revealed the occurrence of broad peaks at higher angles of reflection; data collection were therefore limited to 45°.

The structure was solved by direct and Fourier methods and refined by full-matrix least-squares methods based on F^2 using the programs SHELX-86[41] and SHELXL-93.[42] All non-hydrogen atoms, except the disordered perchlorate oxygen atoms (O(6) and O(7)), were refined anisotropically, while the disordered oxygens were refined isotropically. The hydrogen atoms were placed at the geometrically calculated positions with fixed isotropic thermal parameters. Neutral atom scattering factors and anamolous dispersion terms were taken from the usual sources.[43] The final least-squares refinement ($I > 2.00\sigma(I)$) converged to $R = 0.082$ and $wR2$ (for all data) $= 0.228$, and goodness of fit was 1.067. The maximum and minimum peaks on the final difference Fourier map correspond to 1.228 and −0.759 e Å^{-3}, respectively. All calculations were performed with a Vax 3400 computer.

Results and Discussion

Synthesis and Characterization. A template reaction involving 4-methyl-2,6-diformylphenol, 1,2-diaminoethane, magnesium acetate, and magnesium nitrate in the ratio 2:2:1:1 leads to the formation of a tetraprotonated macrocyclic magnesium

(39) Nanda, K. K.; Mohanta, S.; Flörke, U.; Dutta, S. K.; Nag, K. *J. Chem. Soc., Dalton Trans.* **1995**, 3831.

(40) O'Connor, C. J. *Prog. Inorg. Chem.* **1979**, *2*, 204.

(41) Sheldrick, G. M. SHELXS-86: A Program for Crystal structure Determination, University of Göttingen, Germany, 1986.

(42) Sheldrick, G. M. SHELXL-93. A Program for Crystal structure Refinement, University of Göttingen, Germany, 1993.

(43) Cromer, D. T.; Waber, J. T. *International Tables for X-ray Crystallography*; Kynoch Press: Birmingham, England, 1974; Vol. IV.

Table 2. Electronic and Infrared Spectral Data

compd	λ_{max}, nm (ϵ, M^{-1} cm^{-1})	IR,[a] cm^{-1}
$[Mg_4L^2(NO_3)_2](NO_3)_2\cdot 4H_2O$ (**1**)		1650 (ν(C=N)), 1490, 1385, 1240, 1045, 830 ($\nu(NO_3^-)$)
$[Cu_2L^3(ClO_4)_2]$ (**2**)	365 (8250), 550 (230)[b]	1620 (ν(C=N)), 1110, 1100, 1075, 630 ($\nu(ClO_4^-)$)
$[Ni_4L^1(\mu_2\text{-}NCS)_2(\mu_2\text{-}H_2O)_2](ClO_4)_2\cdot 2CH_3CN$ (**5**)	1120 (35), 875 (50), 620 (70), 350 sh (950)[b]	3240 (ν(NH)), 2020 (ν(NCS)), 1605 (δ(NH))
$[Ni_4L^1(\mu_2\text{-}N_3)_2(\mu_2\text{-}H_2O)_2](ClO_4)_2\cdot 2CH_3OH$ (**6**)	1100 (35), 900 (55), 620 (60), 350 sh (1250)[c]	3240 (ν(NH)), 2040 ($\nu_{as}(N_3^-)$), 1605 (δ(NH))
$[Ni_4L^1(\mu_2\text{-}OAc)_2(\mu_2\text{-}H_2O)_2](ClO_4)_2\cdot 2H_2O$ (**7**)	1190 (30), 905 (50), 625 (70), 370 sh (400)[c]	3280 (ν(NH)), 1610 (δ(NH)), 1570 ($\nu_{as}(CO_2^-)$), 1380 ($\nu_s(CO_2^-)$)
$[Ni_4L^1(\mu_2\text{-}Cl)_2(\mu_2\text{-}H_2O)_2](ClO_4)_2\cdot 4H_2O$ (**8**)	1190 (30), 875 (50), 630 (75), 375 sh (520)[c]	3260 (ν(NH)), 1605 (δ(NH))
$[Ni_3L^1(acac)_2(H_2O)_2](H_2O)_2]\cdot 2H_2O$ (**9**)	990 (45), 630 (20), 355 (70)[d]	3270 (ν(NH)), 1600 (ν(C$\bar{\cdot}\cdot$O)), 1510 (ν(C$\bar{\cdot}\cdot$C))
$[Ni_4L^1(acac)_2(H_2O)_4](ClO_4)_2$ (**10**)	1030 (30), 610 (20), 475 (40)[b]	3260 (ν(NH)), 1595 (ν(C$\bar{\cdot}\cdot$O)), 1515 (ν(C$\bar{\cdot}\cdot$C))

[a] In KBr. [b] In DMF. [c] In MeOH−MeCN (1:1). [d] In $CHCl_3$.

compound of composition $[Mg_2(L^2\text{-}H_4)(NO_3)_2](NO_3)_2\cdot 6H_2O$ (**1**). The IR spectrum (Table 2) of the compound shows a strong band at 1650 cm^{-1} due to the C=N stretching vibration and several bands due to the nitrate ions, of which the bands observed at 1385 and 830 cm^{-1} are attributable to the ionic nitrate, while those at 1490, 1240, and 1045 cm^{-1} due to the coordinating nitrate.[44] The ^{1}H NMR spectrum of the compound provides a clear evidence of its symmetric structure. That the formation of **1** is associated with [4+4] cyclization reaction is established by the fact that **1** on reduction with $NaBH_4$, followed by demetallation with $(EDTA)^{4-}$, affords the 36-membered octaaminotetraphenol macrocyclic ligand H_4L^1 in high overall yield (70%).

Interestingly, **1** on transmetalation with copper(II) perchlorate does not produce a tetracopper(II) complex, but a dicopper(II) complex of composition $[Cu_2L^3(ClO_4)_2]$ (**2**) is obtained. From the X-ray structure determination of **2**[45] it turned out that $(L^3)^{2-}$ is the [2+2] cyclized derivative of 4-methyl-2,6-diformylphenol and 1,2-diaminoethane. Clearly, the conversion of **1** to **2** takes place at the steric requirement of the copper(II) ions, which induces the hydrolytic cleavage of a pair of diagonally opposite CH=N bonds of **1**, followed by the intramolecular amine−aldehyde condensation reaction in the fragments. Complex **2** exhibits the C=N stretching frequency at 1620 cm^{-1}, and the three sharp bands observed in the range 1120−1050 cm^{-1} (Table 2) are due to the coordinated perchlorate. The electronic absorption spectrum of **2** (Table 2) shows a broad d−d band with its maxima at about 550 nm and a phenolate → copper(II) charge transfer transition with its peak at 365 nm.

The redox behavior of **2** has been studied by cyclic voltammetry and differential pulse voltammetry in DMSO solution using glassy carbon working electrode. The reduction of $Cu^{II}Cu^{II}$ to $Cu^{II}Cu^{I}$ takes place reversibly at −0.55 V vs Ag/AgCl, while further reduction to $Cu^{I}Cu^{I}$ occurs irreversibly at −1.12 V. Under similar condition, the dicopper(II) complex $[Cu_2L^4](ClO_4)_2\cdot 2H_2O$ derived from [2+2] condensation of 4-methyl-2,6-diformylphenol and 1,3-diaminopropane exhibits two quasireversible redox couples due to $Cu^{II}Cu^{II}/Cu^{II}Cu^{I}$ and $Cu^{II}Cu^{I}/Cu^{I}Cu^{I}$ at −0.48 and −0.94 V, respectively. In the positive potential range, up to 1.7 V, the electrochemical behavior of both the compounds (MeCN solutions, Pt electrode) were featureless. A negative shift in the first one-electron reduction potential of $[Cu_2L^3]^{2+}$ (−0.555 V) relative to that of $[Cu_2L^4]^{2+}$ (−0.48 V) is indicative of the enhanced stability of copper(II) in **2**.

As reported earlier, the macrocyclic ligand H_4L^1 on reaction with the perchlorate salts of copper(II) and nickel(II) in the presence of triethylamine produce the tetranuclear complexes $[Cu_4L^1(H_2O)_4](ClO_4)_4$ (**3**)[39] and $[Ni_4L^1(\mu_3\text{-}OH)(\mu_2\text{-}H_2O)_2(ClO_4)](ClO_4)_2\cdot 2CH_3COCH_3\cdot H_2O$ (**4**).[37] The hydroxo bridge in the asymmetric complex **4** can be replaced by other bridging anions (X^-) to generate the symmetric core cation $[Ni_4L^1(\mu_2\text{-}X)_2(\mu_2\text{-}H_2O)_2]^{2+}$. Thus, the metathetical reactions between **4** and appropriate salts of the bridging anions (X^- = NCS, N_3, OAc, and Cl) readily afford the hetero-bridged complexes $[Ni_4L^1(\mu_2\text{-}NCS)_2(\mu_2\text{-}H_2O)_2](ClO_4)_2\cdot 2CH_3CN$ (**5**), $[Ni_4L^1(\mu_2\text{-}N_3)_2(\mu_2\text{-}H_2O)_2](ClO_4)_2\cdot 2CH_3OH$ (**6**), $[Ni_4L^1(\mu_2\text{-}OAc)_2(\mu_2\text{-}H_2O)_2](ClO_4)_2\cdot 2H_2O$ (**7**), and $[Ni_4L^1(\mu_2\text{-}Cl)_2(\mu_2\text{-}H_2O)_2]Cl_2\cdot 4H_2O$ (**8**).

The IR and UV−vis spectral data for **5**−**8** are given in Table 2. All of them exhibit a weak ν(NH) vibration in the range 3270−3250 cm^{-1} and a medium intensity δ(NH) vibration between 1610 and 1600 cm^{-1} due to the macrocyclic ligand. The presence of the free perchlorate ions in **5**−**7** are evident from the broad nature of the $\nu_3(ClO_4^-)$ band observed at 1100 cm^{-1}. In **5** a strong band due to the thiocyanate ions (ν(CN)) is observed at 2020 cm^{-1}. Although it is not easy to distinguish different modes of thiocyanate coordination on the basis of ν(CN) frequencies, there are few established cases where ν(CN) of N-bonded bridged-thiocyanate have been reported[47] to occur between 2000 and 2030 cm^{-1}. The presence of the >NCS bridge in **5** has been confirmed by the X-ray structure determination. Complex **6** exhibits a strong band at 2040 cm^{-1} due to $\nu_{as}(N_3^-)$. Again there is no well-defined criterion based on which end-on and end-to-end azido-bridged complexes can be distinguished. Nevertheless, by analogy to **5**, in **6** bridging seems to occur through the N^1 (end-on) nitrogens. It will be seen later that the magnetic properties of **6** is consistent with the end-on bridging. The asymmetric and symmetric carboxylate stretching vibrations in **7** are observed at 1570 and 1380 cm^{-1}, respectively, and their energy difference Δ = 180 cm^{-1}, suggests the presence of bridging acetate.[44]

Complexes **5**−**8** exhibit quite similar absorption spectral features (Table 2) with four peaks around 1200−1100, 900−875, 630−620, and 370−350 nm, which are indicative of low-symmetry six-coordination geometry of the nickel(II) centers.[48] The first two bands appear to be the split components of the spin-allowed $^3A_{2g} \rightarrow {}^3T_{2g}$ transition of octahedral nickel(II), which in D_{4h} symmetry may be attributed to $^3B_{1g} \rightarrow {}^3E_g$ and

(44) Nakamoto, K. *Infrared and Raman Spectra of Inorganic and Coordination Compounds*, 3rd ed.; Wiley: New York, 1978.
(45) Mohanta, S.; Dutta, S. K.; Flörke, U.; Nag, K. Unpublished results.
(46) Mandal, S. K.; Thompson, L. K.; Nag, K.; Charland, J.-P.; Gabe, E. J. *Inorg. Chem.* **1987**, *26*, 1391.
(47) (a) van Albada, G. A.; de Graff, R. A. G.; Haasnoot, J. G.; Reedijk, J. *Inorg. Chem.* **1984**, *23*, 1404. (b) Harding, P. A.; Henrick, K.; Lindoy, L. F.; McPartlin, M.; Tasker, P. A. *J. Chem. Soc., Chem. Commun.* **1983**, 1300. (c) Cotton, F. A.; Davison, A.; Ilsley, W. H.; Trop, H. S. *Inorg. Chem.* **1979**, *18*, 2719.
(48) Lever, A. B. P. *Inorganic Electronic Spectroscopy*, 2nd ed.; Elsevier: Amsterdam, 1984.

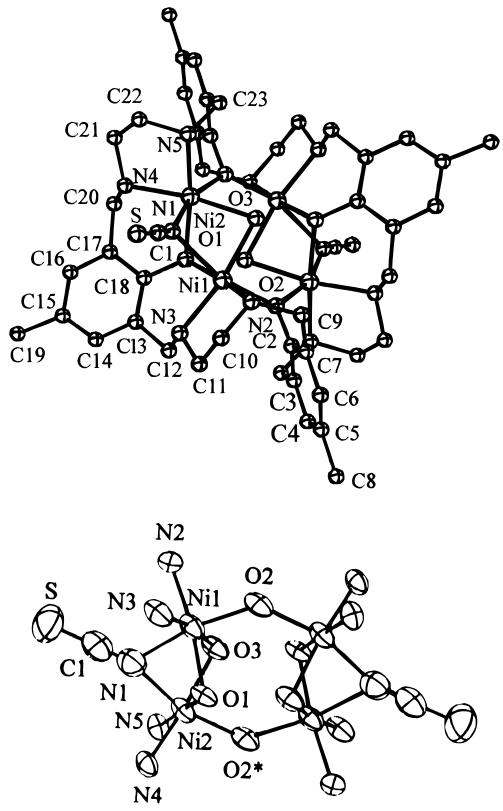

Figure 1. (a) Top: ORTEP plot of the cation $[Ni_4L^1(\mu_2\text{-}NCS)_2(\mu_2\text{-}H_2O)_2]^{2+}$ in **5** showing the 50% probability thermal ellipsoids. (b) Bottom: Inner coordination sphere of the nickel atoms in **5**.

$^3B_{1g} \rightarrow {}^3B_{2g}$ transitions. The remaining two bands are $^3A_{2g} \rightarrow {}^3T_{1g}$ and $^3A_{2g} \rightarrow {}^3T_{1g}(P)$ transitions.

In a previous study the structure of a helically twisted heterotrinuclear complex $[Cu_2Zn(L^1\text{-}H)](ClO_4)_3 \cdot 3H_2O$, which is obtained by reacting $Cu(acac)_2$, H_4L^1, and $Zn(ClO_4)_2 \cdot 4H_2O$, has been reported.[39] When $Ni(acac)_2$ is reacted with H_4L^1, irrespective of the ratio of the reactants, the product obtained has the composition $[Ni_3L^1(acac)_2(H_2O)_2] \cdot 2H_2O$ (**9**). This compound on further reaction with nickel(II) perchlorate forms the tetranuclear complex $[Ni_4L^1(acac)_2(H_2O)_4](ClO_4)_2$ (**10**). In both compounds, the $\nu(C\overset{\cdot\cdot}{-}O)$ and $\nu(C\overset{\cdot\cdot}{-}C)$ vibrations due to the acetylacetonate moieties are observed at about 1600 and 1510 cm^{-1}, respectively. Their electronic spectra show features (Table 2) typical of octahedral nickel(II). The formation of the trinuclear complex **9** is determined by the size of the macrocyclic ligand, which apparently cannot accommodate more than two acetylacetonate moieties. However, there is enough space in the cavity of **9** to accommodate one more nickel(II) ion to produce **10**.

Structure of $[Ni_4L^1(\mu_2\text{-}NCS)_2(\mu_2\text{-}H_2O)_2](ClO_4)_2 \cdot 2CH_3CN$ (5). A perspective view of the cation in **5** along with the atom labels is shown in Figure 1a, and an ORTEP representation of the coordination environment around the nickel centers is illustrated in Figure1b. Atomic coordinates and selected bond distances and angles are given in Table 3 and 4, respectively. The cation has a centrosymmetric structure with its center of inversion at the point of intersection between the lines joining (1) and Ni(1′), and Ni(2) and Ni(2′). In the asymmetric unit the two nickel atoms are triply-bridged by the phenoxide oxygen O(1), the aqua oxygen O(3), and the thiocyanate nitrogen N(1); an additional bridge is provided to each of the metal centers by the phenoxide oxygen O(2) and O(2′). The coordination sphere NiN_3O_3 is completed by two secondary amine nitrogens of the macrocyclic ligand. The equatorial plane of Ni(1) is best described by N(1)N(3)O(2)O(3) atoms; their displacements from the mean plane are within 0.04 Å, while the metal center lies below this plane by 0.09 Å. In the case of Ni(2) an almost exact plane is formed by N(1)N(4)O(2′)O(3), although the metal center is displaced above this plane by 0.10 Å. The dihedral angle between the two planes is 108.6°. On the other hand, the related phenyl rings are inclined to each other by 58.7°.

The Ni−O distances for both the metal centers, irrespective of the equatorial or axial positions, are not much different (average 2.094(10) Å). By contrast, the axial Ni−N(amine) distances (Ni(1)−N(2) = 2.072(9) Å and Ni(2)−N(5) = 2.083(8) Å) are longer relative to the in-plane Ni−N amine distances (Ni(1)−N(3) = 2.048(8) Å and Ni(2)−N(4) = 2.019(8) Å). More significant is the difference between the two Ni−N(1) distances (2.279(10) and 2.146(11) Å) of the bridged-thiocyanate. The *cisoid* angles for the metal centers range from 76.3(3) to 103.1(3)° and the *transoid* angles vary between 162.2(3) and 174.6(3)°, indicating significant distortion of the octahedral geometry of nickel(II). The thiocyanate ion is linear, N(1)−C(1)−S = 178.7(9)°, albeit the nonequivalence of the two Ni−N(1) distances are strongly reflected in corresponding Ni−N(1)−C(1) angles (125.3(7)° for Ni(1) and 152.2(7)° for Ni(2)).

Table 3. Atomic Coordinates ($\times 10^4$) and Equivalent Isotropic Displacement Parameters ($Å^2 \times 10^3$) of **5**[a]

	x	*y*	*z*	U_{eq}
Ni(1)	884(1)	646(1)	3711(1)	56(1)
Ni(2)	−299(1)	−2019(1)	3168(1)	55(1)
Cl	3021(4)	5142(4)	2039(3)	93(1)
S	2161(7)	−1584(5)	531(5)	147(2)
O(1)	−1008(6)	−666(6)	3266(6)	50(2)
O(2)	961(7)	2128(6)	5419(6)	61(2)
O(3)	1293(7)	−273(6)	4628(6)	57(2)
O(4)	3936(14)	5633(12)	1509(13)	156(5)
O(5)	1927(12)	4095(12)	1098(11)	150(6)
O(6A)[b]	2978(24)	6329(21)	3081(20)	128(8)
O(7A)[b]	3634(20)	4691(20)	2553(20)	107(6)
O(6B)[b]	2740(26)	6370(22)	2469(25)	147(9)
O(7B)[b]	3233(24)	5169(24)	3112(19)	130(8)
N(1)	738(12)	−1319(11)	2161(11)	80(3)
N(2)	2708(9)	1800(8)	3876(8)	58(2)
N(3)	351(10)	1186(8)	2523(8)	64(3)
N(4)	−1765(9)	−3507(8)	1616(7)	58(3)
N(5)	344(9)	−3462(8)	2882(8)	57(2)
N(6)	3467(14)	9659(18)	4251(18)	139(7)
C(1)	1304(17)	−1423(13)	1487(15)	84(5)
C(2)	1579(12)	3395(10)	5643(9)	54(3)
C(3)	976(11)	4237(11)	5974(10)	58(3)
C(4)	1592(13)	5506(11)	6147(10)	59(3)
C(5)	2759(15)	5979(11)	6070(10)	69(4)
C(6)	3365(11)	5162(12)	5776(11)	65(3)
C(7)	2785(12)	3853(10)	5570(10)	57(3)
C(8)	3451(13)	7346(11)	6239(12)	78(4)
C(9)	3428(11)	2964(10)	5175(11)	67(3)
C(10)	2623(14)	2189(11)	2950(11)	78(4)
C(11)	1433(13)	2349(12)	2724(12)	73(4)
C(12)	−815(12)	1323(10)	2620(10)	60(3)
C(13)	−1914(11)	−17(10)	1973(9)	55(3)
C(14)	−2921(12)	−347(11)	1050(10)	62(3)
C(15)	−3908(11)	−1594(11)	333(10)	58(3)
C(16)	−3917(11)	−2529(11)	611(10)	62(3)
C(17)	−2957(11)	−2285(10)	1553(9)	59(3)
C(18)	−1930(11)	−964(10)	2275(10)	57(3)
C(19)	−5003(13)	−1954(13)	−711(12)	85(4)
C(20)	−2957(12)	−3412(10)	1696(10)	60(3)
C(21)	−1801(13)	−4821(11)	1318(10)	68(4)
C(22)	−476(13)	−4639(11)	1642(11)	72(4)
C(23)	295(13)	−3781(11)	3896(10)	66(4)
C(24)	4105(21)	9320(20)	3573(24)	136(8)
C(25)	4914(17)	8877(17)	2870(17)	115(6)

[a] U_{eq} is defined as one-third of the trace of the orthogonalized $\mathbf{U}_{ij}$ tensor. [b] Occupancy factor 0.5.

Table 4. Selected Bond Distances (Å) and Angles (deg) for $[Ni_4L^1(\mu_2\text{-}NCS)_2(\mu_2\text{-}H_2O)_2](ClO_4)\cdot 2CH_3CN$ (**5**)

Ni(1)−N(3)	2.048(8)	Ni(2)−N(4)	2.019(8)
Ni(1)−N(2)	2.027(9)	Ni(2)−N(5)	2.083(8)
Ni(1)−O(2)	2.087(7)	Ni(2)−O(1)	2.094(6)
Ni(1)−O(3)	2.105(6)	Ni(2)−O(2′)	2.088(8)
Ni(1)−O(1)	2.102(7)	Ni(2)−O(3)	2.124(7)
Ni(1)−N(1)	2.279(10)	Ni(2)−N(1)	2.146(11)
Ni(1)···Ni(2)	2.845(2)	Ni(1)···Ni(2′)	3.808(3)
N(2)−Ni(1)−N(3)	84.1(4)	N(4)−Ni(2)−N(5)	85.4(3)
N(3)−Ni(1)−O(2)	103.1(3)	N(4)−Ni(2)−O(2′)	103.2(3)
N(2)−Ni(1)−O(2)	92.7(3)	N(5)−Ni(2)−O(2′)	91.9(3)
N(2)−Ni(1)−O(3)	99.9(3)	N(5)−Ni(2)−O(3)	100.4(3)
N(3)−Ni(1)−O(1)	90.9(3)	N(4)−Ni(2)−O(1)	90.1(3)
N(3)−Ni(1)−N(1)	93.5(3)	N(4)−Ni(2)−N(1)	92.5(4)
N(2)−Ni(1)−N(1)	95.5(4)	N(5)−Ni(2)−N(1)	95.6(4)
O(2)−Ni(1)−O(3)	86.7(3)	O(2)−Ni(2)−O(3)	85.0(3)
O(1)−Ni(1)−O(2)	94.6(3)	O(1) −Ni(2)−O(2′)	91.9(3)
O(1)−Ni(1)−O(3)	83.9(3)	O(1)−Ni(2)−O(3)	83.6(2)
O(3)−Ni(1)−N(1)	76.3(3)	O(3)−Ni(2)−N(1)	78.9(3)
O(1)−Ni(1)−N(1)	78.4(3)	O(1)−Ni(2)−N(1)	81.7(3)
O(1)−Ni(1)−N(2)	171.9(3)	O(1)−Ni(2)−N(5)	174.6(3)
O(3)−Ni(1)−N(3)	169.3(3)	O(3)−Ni(2)−N(4)	169.9(3)
O(2)−Ni(1)−N(1)	162.2(3)	O(2′)−Ni(2)−N(1)	163.1(3)
Ni(1)−O(1)−Ni(2)	85.3(3)	Ni(1)−O(3)−Ni(2)	84.5(2)
Ni(1)−O(2)−Ni(2′)	131.6(3)	Ni(1)−N(1)−Ni(2)	80.0(4)
Ni(1)−N(1)−C(1)	125.3(7)	Ni(2)−N(1)−C(1)	152.2(7)
N(1)−C(1)−S	178.7(9)		

In the asymmetric unit the bridge angles involving one of the phenoxides (Ni(1)−O(1)−Ni(2) = 85.3(3)°), the water molecule (Ni(1)−O(3)−Ni(2) = 84.5(2)°), and the thiocyanate (Ni(1)−N(1)−Ni(2) = 80.0(4)°) lie within a small range. On the other hand, the phenoxide bridge angle involving the symmetry related units is much wider (Ni(1)−O(2)−Ni(2′) = 131.6(3)°). It should be noted that these Ni−O−Ni angles are quite different from the values (99−106°) reported for several dinickel(II) complexes[7,49] derived from a binucleating propane-bridged tetraaminodiphenol macrocyclic ligand. The nonbonded distances between the metal centers in **5** are: Ni(1)···Ni(2) = 2.845(2) Å and Ni(1)···Ni(2′) = 3.808(3) Å.

Magnetic Properties. The variable-temperature (4−300 K) magnetic susceptibility data were collected for powdered samples of **3**−**8**. The variations of molar magnetic susceptibility (χ_M) and magnetic moment (μ_{eff}) with temperature for some of these compounds are illustrated in Figures 2−5. The exchange coupling constants (*J*'s) and other relevant parameters of these compounds obtained by analyzing the magnetic susceptibility data using the Heisenberg Hamiltonian (eq 1) are given in Table 5.

$$H = -2\sum_{j>i=1}^{4} J_{ij} S_i \cdot S_j \qquad (1)$$

In order to understand the magnetic properties of the tetranuclear complexes three spin interaction schemes (**I**−**III**, shown in Chart 2) have been considered. Assuming that the $[Ni_4L^1(\mu_2\text{-}X)_2(\mu_2\text{-}H_2O)_2]^{2+}$ cations in **5**−**8** have related structures, the mode of exchange coupling in them can be described by **I**. Complex **4**, $[Ni_4L^1(\mu_3\text{-}OH)(\mu_2\text{-}H_2O)_2(ClO_4)](ClO_4)_2\cdot 2CH_3COCH_3\cdot H_2O$, has been shown[7] to have a nonsymmetrical structure in which each of the metal centers are bridged by a pair of phenoxides; moreover, while three of these metals are anchored by the hydroxyl group, the two metal pairs are linked by the two aqua bridges. Although spin coupling in **4**, in principle, involves five different pathways, to be realistic,

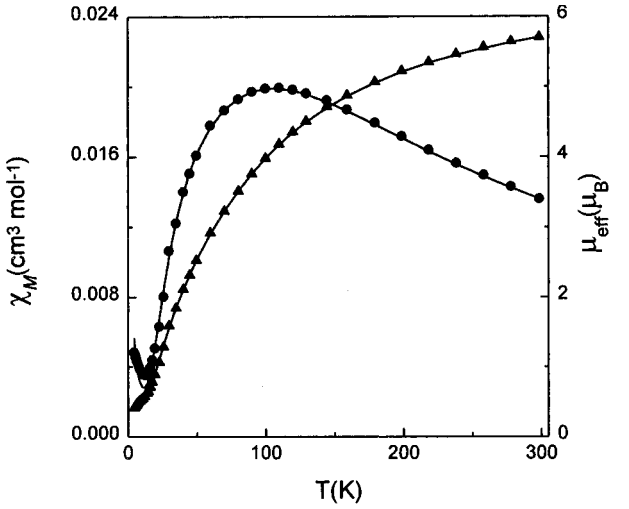

Figure 2. Thermal variations of experimental molar magnetic susceptibility (●) and effective magnetic moment (▲) for **5**. The solid lines are the calculated values using the best-fit parameters given in Table 5.

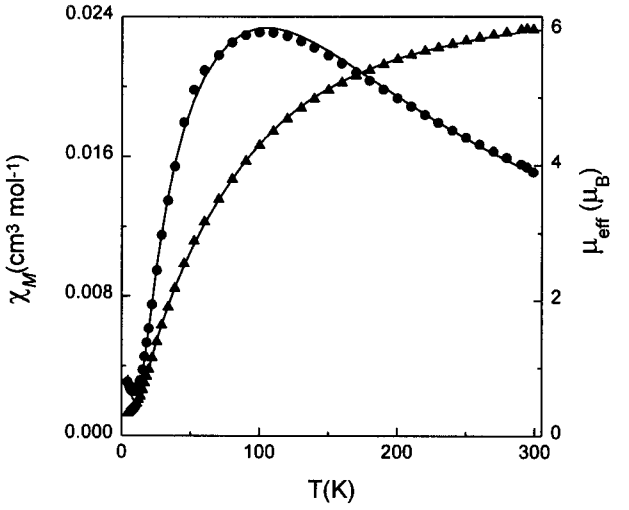

Figure 3. Thermal variations of experimental molar magnetic susceptibility (●) and effective magnetic moment (▲) for **6**. The solid lines are the calculated values using the best-fit parameters given in Table 5.

exchange interactions have been modeled as **II** by considering only two *J*'s. Finally, the exchange interaction in $[Cu_4L^1(H_2O)_4](ClO_4)_4$ (**3**) has been modeled as **III** by considering a single *J* because each of the metal centers are bridged by a pair of phenoxides only.

In the case of model **I** eq 1 can be rewritten as

$$H = -2J_1(S_1\cdot S_2 + S_3\cdot S_4) - 2J_2(S_1\cdot S_4 + S_2\cdot S_3) \qquad (2)$$

where $J_1 = J_{12} = J_{34}$ corresponds to the interaction between the pair of metal ions bridged by a phenoxide group alone and $J_2 = J_{23} = J_{34}$ indicates the spin exchange integral involving the triply-bridged metal ion pair. It is important to note that the Hamiltonian in eq 2 is symmetric; therefore, the assignment of J_1 to the interaction between S_1 and S_2 is arbitrary. It could as well be between S_1 and S_4. However, on the basis of a known magneto−structural relationship of phenoxo-bridged nickel(II) complex,[7] J_1 has been considered to represent the more antiferromagnetic interaction involving the wider Ni−O(phenoxo)−Ni bridge angle. A 81 × 81 spin wave function matrix under Hamiltonian (2) has been diagonalized numerically in blocks to obtain energies $E(S_T)$ of 19 eigenstates, which on substitution

(49) Nanda, K. K.; Das, R.; Thompson, L. K.; Venkatsubramanian, K.; Paul, P.; Nag, K. *Inorg. Chem.* **1994**, *33*, 1188 and references therein.

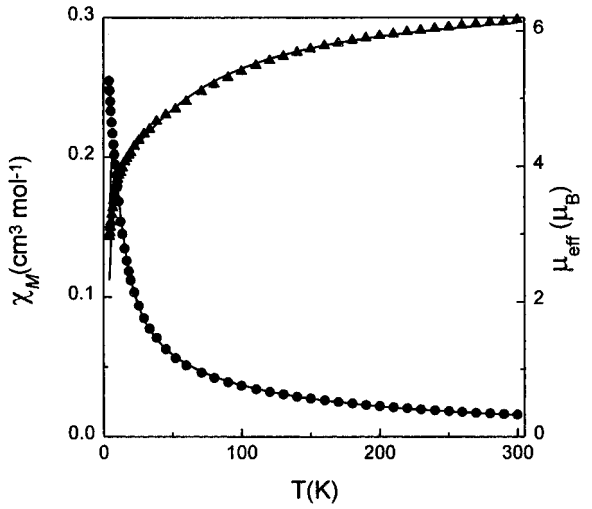

Figure 4. Thermal variations of experimental molar magnetic susceptibility (●) and effective magnetic moment (▲) for **4**. The solid lines are the calculated values using the best-fit parameters given in Table 5.

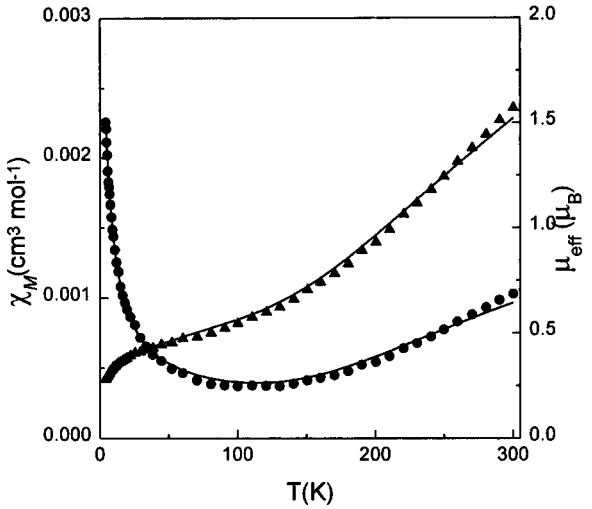

Figure 5. Thermal variations of experimental molar magnetic susceptibility (●) and effective magnetic moment (▲) for **3**. The solid lines are the calculated values using the best-fit parameters given in Table 5.

Table 5. Magnetic Data for the Complexes

complex	J_1, cm^{-1}	J_2, cm^{-1}	g	p^a
3[b]	−288(2)		2.18(2)	0.034
4[c]	−8.1(2)	−10.2(2)	2.26(2)	0.010
5[c]	−34.5(1.0)	−9.5(2.0)	2.33(2)	0.017
6[c]	−34(1)	11(2)	2.32(2)	0.010
7[c]	−30(1)	−7.0(1.5)	2.35(2)	0.015
8[c]	−32(1)	−4(1)	2.37(2)	0.040

[a] Mole fraction of mononuclear paramagnetic impurity. [b] TIP = 240 × 10^{-6} cm^3 mol^{-1}. [c] TIP = 400 × 10^{-6} cm^3 mol^{-1}.

to the van Vleck eq 3 gives the theoretical expression of

$$\chi_{M'} = \frac{N\beta^2 g^2}{3kT} \frac{\sum_{S_T} S_T(S_T+1)(2S_T+1)e^{-E(S_T)/kT}}{\sum_{S_T}(2S_T+1)e^{-E(S_T)/kT}} \qquad (3)$$

$$\chi_M = \chi_{M'}(1-p) + \frac{2N\beta^2 g^2 p}{3kT} + \text{TIP} \qquad (4)$$

magnetic susceptibility. Equation 3 has been modified to eq 4

Chart 2

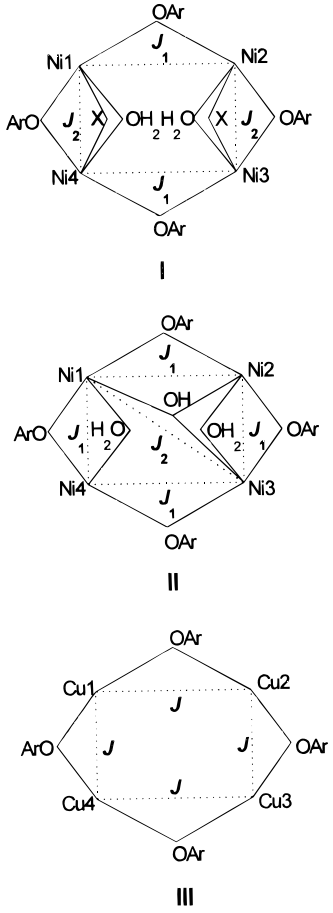

to include the contribution of the uncoupled species (p, mole fraction), assuming to follow a Curie law, and temperature-independent paramagnetism (TIP); N, β, g, k, and T have their usual meanings. Nonlinear least-squares fittings of the theoretical expression to the experimental data have been made by varying J_1, J_2, g, and p and minimizing the residual $R = [\sum(\chi_{obs} - \chi_{calc})^2/\sum(\chi_{obs})^2]$.

The thermal dependencies of χ_M and μ_{eff} for **5** and **6** are shown in Figures 2 and 3. In both the cases, lowering of temperature leads χ_M to increase to reach a maximum at 110 K for **5** and 100 K for **6**, below which temperatures χ_M rapidly decreases to reach a minimum at about 11 K for **5** and 7.5 K for **6**. The increase of χ_M on further lowering of temperature can be attributed to the presence of a small amount of paramagnetic impurity. Corresponding μ_{eff} vs T plots show steady decrease of the magnetic moment from 5.70 μ_B at 298.4 K to 0.41 μ_B at 4.4 K for **5**, while the decrease is from 6.01 to 0.33 μ_B for **6**. Complexes **7** and **8** behave in the same way with their maxima occurring in χ_M vs T plots at 90 and 95 K, respectively. Clearly, the overall magnetic exchange interaction in **5**−**8** is antiferromagnetic and the spin ground state is singlet.

In order to simulate the χ_M (or μ_{eff}) vs T plots of **5**−**8**, initially these systems were treated as independent dimers. However, no satisfactory least-squares fits were obtained. In the second step, J_1 and J_2 were considered to be equal, which again could not reproduce the experimental curves reasonably. Finally, when all the four parameters (J_1, J_2, g, and p) were allowed to vary freely, excellent fits were obtained (as shown in Figures 2 and 3). The best fit parameters thus obtained are as follows: $J_1 = -34.5$ cm^{-1}, $J_2 = -9.5$ cm^{-1}, $g = 2.33$, $p = 0.017$, and $R = 0.73 \times 10^{-3}$ for **5**; $J_1 = -34.0$ cm^{-1}, $J_2 = 11.0$ cm^{-1}, $g = 2.32$, $p = 0.010$, and $R = 0.28 \times 10^{-3}$ for **6**; $J_1 = -30.0$

cm^{-1}, $J_2 = -7.0$ cm^{-1}, $g = 2.35$, $p = 0.015$, and $R = 0.77 \times 10^{-3}$ for **7**; $J_1 = -32.0$ cm^{-1}, $J_2 = -4.0$ cm^{-1}, $g = 2.38$, $p = 0.040$, and $R = 2.51 \times 10^{-3}$ for **8**. To be sure that in all the cases global minima have been reached, the minimum value of the error residual (R) was searched by varying both J_1 and J_2 in the range -50 to $+50$ cm^{-1}, while keeping g and p fixed. The combination of J_1 and J_2 given above, indeed, gave the minimum value of R, albeit the dependency of R on J_1 is more prominent relative to that on J_2. Typically, uncertainty of J_1 is about 3%, while that of J_2 may be as high as 25%.

A comparison of the exchange coupling constants of **5**−**8** (Table 5) indicates that the overall antiferromagnetic behavior exhibited by the compounds is due to the domineering influence of J_1. The values of J_1, however, do not vary substantially in the series ($-34.5(1.0)$ to $-30(1)$ cm^{-1}). In a previous study with diphenoxo-bridged binuclear nickel(II) complexes, it has been shown[7] that the value of $-J_1$ increases with the increase of Ni−O−Ni bridge angle and for 1° variation of angle the change of J is -7.2 cm^{-1}. Although this magneto−structural relation is not applicable to **5**−**8** due to differences in structural arrangements of the metal centers in two cases, the small variation of J_1 may be associated with small differences in the wider Ni−O−Ni bridge angle of these compounds. In contrast to the J_1 values, more significant differences occur with the J_2 values, for which even the change of sign takes place. Thus, while J_2 is antiferromagnetic for **5** ($-9.5(2.0)$ cm^{-1}), **7** (-7.0-(1.5) cm^{-1}), and **8** ($-4(1)$ cm^{-1}), it is ferromagnetic for **6** (11-(2) cm^{-1}).

It is not easy to predict the sign and the magnitude of J_2. In the first place, for this pair of the nickel(II) centers interactions take place through the Ni−X−Ni, Ni−OH_2−Ni, and Ni−OAr−Ni bridges, which contribute differently to J_2. Second, since these two metal centers are noncoplanar, different orientations of the two pairs of magnetic orbitals ($d_{x^2-y^2}$ and d_{z^2}) involved therein complicate the matter.

Little is known about magnetic properties of N-bonded μ_2-NCS nickel(II) complexes, except weak ferromagnetism reported in a trinuclear compound.[47a] A previous study with dinickel-(II) complexes having both phenoxide and carboxylate bridges has indicated[50] that the sign of J can be either positive or negative, but in any case the interaction is weak. The magneto−structural data available for a few chloro-bridged nickel(II) complexes[51] are indicative of ferromagnetic interactions. More definitive results are accessible for azido-bridged nickel(II) complexes. Compounds with end-on bridge are known to exhibit ferromagnetic exchange,[9a,52] while end-to-end bridge systems give rise to antiferromagnetic interaction.[9b,53] For several end-on μ_2-N_3 nickel(II) complexes J values have been reported[52] to lie in the range 20−49 cm^{-1}. In light of the above facts the decreased order of antiferromagnetic interaction ($-J_2$) **5** > **7** > **8** does not appear unusual. Substantial ferromagnetic interaction in **6** ($J_2 = 11(2)$ cm^{-1}) is quite significant. Clearly, the azide bridge in **6** is end-on type; the sign and the magnitude of J_2 is determined by the domineering influence of the interaction occurring through the Ni−N(N_3^-)−Ni bridge. To get an idea about the spin-manifolds in two compounds with different signs of J_2, the $E(S_T)$ values of **5** and **6** are presented in Figure 6. For both compounds the spin ground state ($S_T = 0$, $E(S_T) = -290$ cm^{-1}) is separated from the next higher spin state ($S_T = 1$) by about 50 cm^{-1} due to the almost identical values of J_1 ($-34.5(1.0)$ cm^{-1} for **5**, $-34(1)$ cm^{-1} for **6**); however, major differences occur in the spin-ladder of the two compounds when $E(S_T)$ values are greater than -180 cm^{-1}.

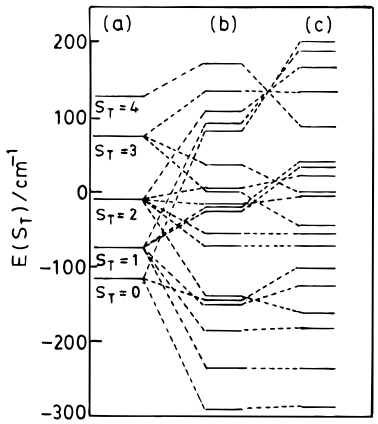

Figure 6. Spin-ladder energies for tetranuclear nickel(II) complexes: (a) A hypothetical system for which all J's are equally antiferromagnetic (energies not to scale); (b) complex **5** with $J_1 = -34.5$ cm^{-1} and $J_2 = -9.5$ cm^{-1}; (c) complex **6** with $J_1 = -34.0$ cm^{-1} and $J_2 = 11$ cm^{-1}.

The spin Hamiltonian for model **II** can be written as

$$H = -2J_1(S_1 \cdot S_2 + S_2 \cdot S_3 + S_3 \cdot S_4 + S_4 \cdot S_1) - 2J_2(S_1 \cdot S_3) \quad (5)$$

where J_1 corresponds to the interaction between the adjacent metal centers and J_2 to the interaction between the diagonal metal centers Ni(1) and Ni(3). By the defining of $S_{13} = S_1 + S_3$, $S_{24} = S_2 + S_4$ and $S_T = S_{13} + S_{24}$ (where $S_1 = S_2 = S_3 = S_4 = S = 1$), the vector coupling method[17,18] allows the spin Hamiltonian of eq 5 to be written in an equivalent operator form and leads to an expression for the energies of eigenstates (eq 6). The theoretical expression for χ_M is obtained, as before,

$$E(S_T,S_{13},S_{24}) = J_1[S_T(S_T+1) - S_{13}(S_{13}+1) - S_{24}(S_{24}+1)] - J_2[S_{13}(S_{13}+1) - 2S(S+1)] \quad (6)$$

using eq 3 and 4. Again there are 19 spin states involving S_{13}, $S_{24} = 2$, 1, 0 and S_T varying from $|S_{13} + S_{24}|$ to $|S_{13} - S_{24}|$ in integer increments.

The cryomagnetic behavior of **4** (Figure 4) shows that χ_M continuously increases with lowering of temperature, while the value of μ_{eff} drops from 6.17 μ_B at 300 K to 2.96 μ_B at 4.3 K. The trend of very rapid decrease of μ_{eff} in the lower temperature range indicates a singlet ground state. The least-squares fit parameters obtained are $J_1 = -8.1$ cm^{-1}, $J_2 = -10.2$ cm^{-1}, $g = 2.26$, $p = 0.026$, and $R = 2.62 \times 10^{-3}$. Error analysis indicated, unlike the previous systems, both J_1 and J_2 are responsive to small variations and the uncertainty is within 3%.

Model **III** for the tetracopper(II) complex **3** takes into consideration pairwise interaction occurring through a phenoxide bridge. Any through-space interaction involving the $d_{x^2-y^2}$ orbital seems unlikely. The spin Hamiltonian in this case is given by eq 7, where $S_A = S_1 + S_3$, $S_B = S_2 + S_4$, $S_T = S_A +$

(50) Nanda, K. K.; Das, R.; Thompson, L. K.; Venkatsubramanian, K.; Nag, K. *Inorg. Chem.* **1994**, *33*, 5934.
(51) (a) Ginsberg, A.; Martin, R. L.; Brookes, R. W.; Sherwood, R. C. *Inorg. Chem.* **1972**, *11*, 2884. (b) Laskowski, E. J.; Felthouse, T. R.; Hendrickson, D. N.; Long, G. *Inorg. Chem.* **1976**, *15*, 2908. (c) Knetsch, D.; Gronveld, W. L. *Inorg. Nucl. Chem. Lett.* **1976**, *12*, 27. (d) Journaux, Y.; Kahn, O. *J. Chem. Soc., Dalton Trans.* **1979**, 1575.
(52) (a) Ribas, J.; Monfort, M.; Diaz, C.; Bastos, C.; Solans, X. *Inorg. Chem.* **1994**, *33*, 484. (b) Vicente, R.; Escuer, A.; Ribas, J.; Fallah, M. S.; Solans, X.; Font-Bardia, M. *Inorg. Chem.* **1993**, *32*, 1920. (c) Arriortua, M. I.; Cortes, A. S.; Lezama, L.; Rojo, T.; Solans, X. *Inorg. Chim. Acta* **1990**, *174*, 263. (d) Escuer, A.; Vicente, R.; Ribas, J. *J. Magn. Mater.* **1992**, *110*, 181.
(53) (a) Pierpont, C. G.; Hendrickson, D. N.; Duggan, D. M.; Wagner, F.; Barefield, E. K. *Inorg. Chem.* **1975**, *14*, 604. (b) Cortes, R.; Urtiaga, M. K.; Lezama, L.; Pizarro, J. L.; Goni, L.; Arriortua, M. I.; Rojo, T. *Inorg. Chem.* **1994**, *33*, 4009. (c) Ribas, J.; Monfort, M.; Diaz, C.; Bastos, C.; Mer, C.; Solans, X.; *Inorg. Chem.* **1995**, *34*, 4986.

$$H = -2J_1(S_1 \cdot S_2 + S_2 \cdot S_3 + S_3 \cdot S_4 + S_4 \cdot S_1) \quad (7)$$

S_B, and $S = {}^1/_2$. There are six eigenstates ($S_T = 2, 1, 1, 1, 0, 0$) whose energies are given by eq 8.

$$E(S_T,S_A,S_B) = -J[S_T(S_T + 1) - S_A(S_A + 1) - S_B(S_B + 1)] \quad (8)$$

The susceptibility can be expressed theoretically:

$$\chi_M = \frac{N\beta^2 g^2}{kT} \frac{4 + 10e^{2x} + 2e^{-2x}}{7 + 5e^{2x} + 3e^{-2x} + e^{-4x}}(1 - p) + \frac{N\beta^2 g^2 p}{4k(T - \Theta)} + \text{TIP} \quad (9)$$

$$x = J/kT$$

The χ_M vs T and μ_{eff} vs T plots for **3**, as shown in Figure 5, are typical of copper(II) complexes exhibiting fairly strong antiferromagnetic exchange interaction. Least-squares fitting of the experimental data gives $J_1 = -288$ cm^{-1}, $g = 2.18$, and $R = 0.54 \times 10^{-3}$. To account for the increase in the χ_M values at lower temperatures the presence of an impurity ($p = 0.034$) obeying the Curie−Weiss law with $\Theta = -3.45$ K has been considered. Subsequently, the possibility of diagonal interaction ($J_2 = J_3 = J_{24}$) has also been considered. However, the susceptibility data have been found to be insensitive to J_2 when it is varied between 0 and -10 cm^{-1}. The magnetic property of **3** is generally in accord with the behavior of copper(II) complexes of the binucleating tetraaminodiphenol and tetraiminodiphenol macrocyclic ligands, albeit for the dicopper(II) compounds antiferromagnetic exchange interactions are stronger ($-J = 360-410$ cm^{-1}).[54]

Acknowledgment. K.N. thanks the Department of Science and Technology, Government of India, for financial support. He is also thankful to Dr. P. Ghosh and Dr. S. Dutta for collecting X-ray data for **5** at the National Single Crystal Diffractometer facility established at IACS, Calcutta.

Supporting Information Available: Tables of crystal data and structure refinement (Table S1), anisotropic thermal parameters (Table S2), complete bond lengths and angles (Table S3), hydrogen atom coordinates (Table S4), and equations of planes (Table S5) for **5** and tables of experimental and calculated χ_M and μ_{eff} values of **5** (Table S6) and **6** (Table S7) in the temperature range 4−300 K (13 pages). Ordering information is given on any current masthead pages.

IC9611103

(54) (a) Mandal, S. K.; Thompson, L. K.; Nag, K.; Charland, J.-P.; Gabe, E. J. *Inorg. Chem.* **1987**, *26*, 1391. (b) Mandal, S. K.; Thompson, L. K.; Nag, K.; Charland, J.-P.; Gabe, E. J. *Can. J. Chem.* **1987**, *65*, 2815. (c) Mandal, S. K.; Thompson, L. K.; Newlands, M. J.; Gabe, E. J.; Nag, K. *Inorg. Chem.* **1990**, *29*, 1324.